Key Points:
- We provide for the first time observation of the latitudinal four-peak structure of F region electron density at the nightside ionosphere
- The latitudinal four-peak structure can persist throughout the night until sunset hours
- We suggest that the enhanced meridional wind at post-midnight hours is one possible driver for causing such latitudinal four-peak structure.

Correspondence to:
C. Xiong,
bear@gfz-potsdam.de

Long-Lasting Latitudinal Four-Peak Structure in the Nighttime Ionosphere Observed by the Swarm Constellation

Chao Xiong[1] , Hermann Lühr[1] , Longchang Sun[2] , Weihua Luo[3] , Jaeheung Park[4,5] , and Yu Hong[2,6]

[1]Section 2.3, Geomagnetism, GFZ German Research Centre for Geosciences, Potsdam, Germany, [2]State Key Laboratory of Space Weather, National Space Science Center, Chinese Academy of Sciences, Beijing, China, [3]College of Electronic and Information Engineer, South Central University for Nationalities, Wuhan, China, [4]Korea Astronomy and Space Science Institute, Daejeon, South Korea, [5]Department of Astronomy and Space Science, University of Science and Technology, Daejeon, South Korea, [6]College of Earth Sciences, University of Chinese Academy of Sciences, Beijing, China

Abstract In this study, we provide for the first time observation of the latitudinal four-peak structure of *F* region electron density in the nightside ionosphere. The special configuration of Swarm satellites, Swarm B having the chance to resample the regions of Swarm A/C with successively increasing time differences, provides an unprecedented opportunity to check the evolution of these nightside electron density peaks. Overall, the latitudinal four-peak structures have very low occurrence rates, only 4% of the Swarm orbits. The two mid-latitude peaks prefer to appear close to ±40° magnetic latitude, while the two low-latitude peaks appear within ±20° magnetic latitude. Such latitudinal four-peak structures can persist throughout the night until sunrise hours. No clear seasonal dependence is found for the two mid-latitude peaks, while the two low-latitude peaks are almost symmetric about the magnetic equator during equinoxes but are located at slightly higher latitudes in the summer hemisphere around solstices. The two low-latitude peaks at late-night hours are believed not to be remnants of the dusk-side equatorial ionization anomaly (EIA) crests, as (a) example shows that Swarm A/C observe the development of shoulders at the flanks of the two EIA crests after sunset hours, and the shoulders become peaks 3 h later when Swarm B resamples the same region; (b) statistic results reveal that the two low-latitude peaks during post-midnight hours do not propagate towards the magnetic equator, as expected for EIA crests, but move slowly poleward. We suggest that the enhanced meridional wind at postmidnight hours is one possible driver for causing such latitudinal four-peak structure of *F* region electron density. In addition, the simultaneous magnetic measurements from Swarm satellites are also analyzed, but they show no obvious diamagnetic effect that could help to maintain pressure balance within these electron density peaks.

1. Introduction

A well-known phenomenon of the low-latitude ionospheric *F* region during daytime is the equatorial ionization anomaly (EIA), which is characterized by an electron density trough above the magnetic equator and double crests of enhanced electron density at about 15° north and south (e.g., Appleton, 1946; Liang, 1947; Namba & Maeda, 1939). The daytime EIA is thought to be driven by the equatorial plasma fountain effect. In the equatorial region the magnetic field lines are primarily horizontal, pointing northward, and the daytime eastward electric field drives the plasma upward via E × B drift. Due to gravitational and pressure gradient forces, the uplifted plasma at higher altitudes eventually diffuses poleward and sediments down along the geomagnetic field lines into both hemispheres, forming the two density crests (Duncan, 1959). The two EIA crests typically appear at about 09:00 local time (LT) and move poleward with a speed of about 1° in latitude per hour for the next few hours (Yeh et al., 2001). The crest-to-trough ratio (CTR) of EIA gradually increased from morning to noon hours and reached the maximum value between 18:00 and 20:00 LT, with a value almost twice the daytime level (e.g., Liu et al., 2007; Xiong et al., 2013). The rapidly increasing CTR value after sunset hours is primarily related to the prereversal enhancement (PRE), which is defined as a sharp increase of plasma vertical drift after sunset via an enhancement of the eastward electric field in the ionospheric *F* region. The *F* region dynamo, driven by the thermospheric zonal wind in the upper

atmosphere, in combination with the conductivity contrast across the day-night terminator, is accepted for causing the PRE (e.g., Eccles et al., 2015; Kelley, 2009).

Previous studies related to EIA focused mainly on its morphology during daytime and shortly after sunset hours. However, its evolution and related mechanism at postmidnight hours have not been well addressed. Woodman (1970) reported postmidnight EIA feature during magnetically disturbed periods from radar observations. Wang et al. (2008) suggested that the disturbed electric fields during storm or substorm periods could produce upward plasma drift, forming the EIA at late night hours. However, McDonald et al. (2008) found that during geomagnetically quiet periods the enhanced EIA during PRE hours could sometimes also last to postmidnight hours. Yizengaw et al. (2009) argued that the two peaks of EIA during postmidnight hours at quiet periods are not the remains from sunset hours; instead, they are caused by the reversed vertical upward drifts related to the F region wind dynamo at postmidnight hours. Therefore, the generation of the postmidnight EIA, especially during magnetically quiet time, is still an open issue.

By using occultation measurements from the Constellation Observing System for Meteorology, Ionosphere, and Climate (COSMIC) satellites, Zhong et al. (2019) showed that the nighttime electron densities at $\pm40°$ magnetic latitude (MLAT) are generally larger during equinoxes, forming two bands at all longitudes; while during solstices the band in the winter hemisphere is much more visible. This nighttime ionospheric band structure at middle latitudes should be the same phenomena as earlier reported nighttime enhancements of the F2 electron density peak, NmF2 (e.g., Arendt & Soicher, 1964; Balan & Rao, 1987; Jakowski & Förster, 1995), which are also more often observed in the winter hemisphere and are suggested to be caused by the enhanced equatorward meridional wind and downward diffusion from the plasmasphere at nighttime (Mikhailov et al., 2000; Zhong et al., 2019).

Until now, there has been no study to put the postmidnight electron density peaks at low and middle latitudes together, and to investigate the possible connection between these peaks. In this study, we use the in situ electron density measurements from the Swarm constellation at altitudes of about 450–510 km, to investigate the nightside ionosphere at both low and middle latitudes. Compared to the ground-based and COSMIC occultation measurements, the Swarm satellites provide a good opportunity for investigating the latitudinal distributions of the ionosphere, as they are flying on circular and polar orbits. Swarm satellites sample the F region ionosphere with an orbital velocity of about 7.5 km/s, almost along the same magnetic meridian in the southern and northern hemispheres within less than 30 min. Within such a short period, the large-scale ionospheric structures, like the EIA, are not expected to change significantly. The Swarm's in situ measurements show that two electron density peaks at low latitudes are still discernable during postmidnight hours, and the other two peaks are sometimes also observed at northern and southern middle latitudes, forming a latitudinal four-peak structure in the nightside ionosphere. With the slowly increasing LT separation between Swarm A/C and Swarm B orbits, we can address the temporal evolution of the latitudinal four-peak structure in more details and the possible relation between these four peaks.

In the sections to follow, we will first introduce the data set, and then provide observations of examples and present statistics of the latitudinal four-peak structure. Finally, we provide relevant discussion by considering previous publications.

2. Data Set

The Swarm mission, comprising three spacecraft, was launched on 22 November 2013 into a near-polar orbit with an initial altitude of about 500 km. During the early months, the three satellites orbited in a string-of-pearls configuration. After a commissioning phase, the final constellation was achieved on 17 April 2014. Two of the Swarm spacecraft, A and C, fly side-by-side at about 460 km altitude, separated by 1.4° of geographic longitude in an east-west direction, and the third, Swarm B, flies at an orbit about 50 km higher. Such a special configuration of satellites permits us to investigate the spatial structure of electron density. More details about the evolution of Swarm configuration can be found in Xiong et al. (2016). In this study, we use the in situ electron density measured by the Swarm onboard Langmuir probe with a time resolution of 2 Hz.

In addition, the global TEC map has been used for comparison. The TEC map is generated based on measurements of a global network of the international GNSS services (IGS), and is provided as a routine
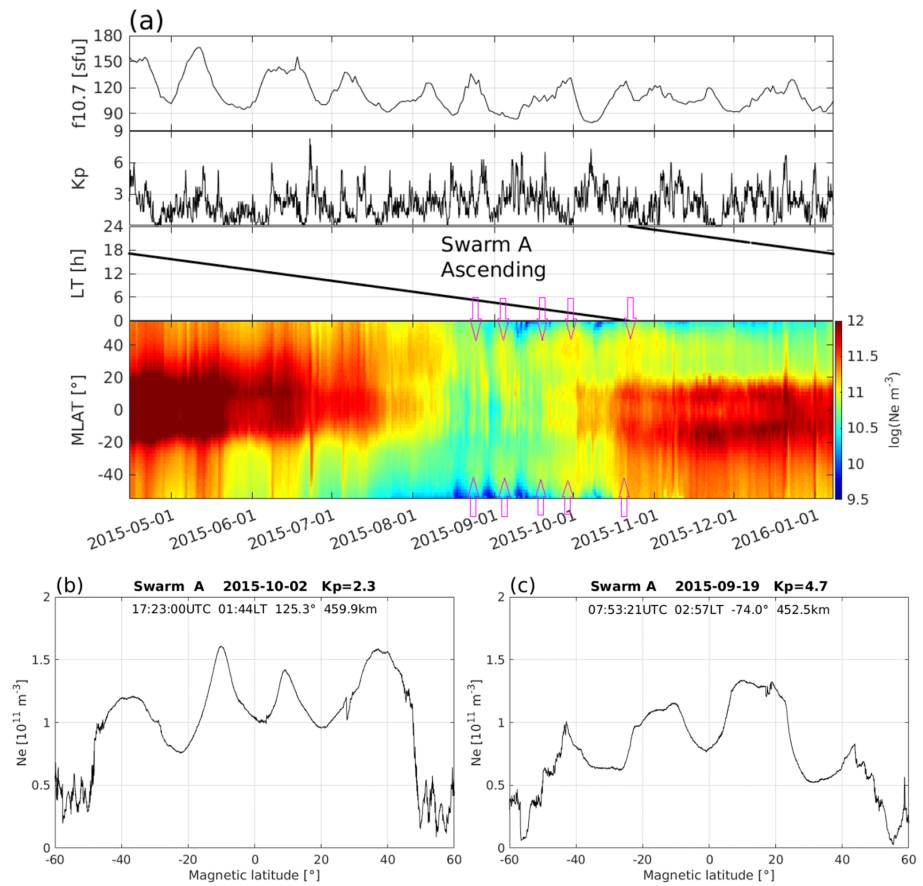
Figure 1. (a) The solar flux index, *f10.7*, magnetic activity index, *Kp*, local time of Swarm A descending orbit, as well as magnetic latitude (MLAT) versus time distribution of Swarm A in situ electron density measurements from 15 April 2015 to 6 January 2016. One electron density profile with four peaks observed by Swarm A during (b) magnetic quiet period on 02 October 2015 and (c) magnetic disturbed period on 19 September 2015.

product by the Chinese Academy of Sciences, with a time cadence of 15 min and a spatial resolution of 2.5° × 5° (geographic latitude versus geographic longitude). For a more detailed description of this TEC product, readers are suggested to refer to Feltens and Schaer (1998) as well as Li et al. (2017).

3. Observations

3.1. Examples of Latitudinal Four-Peak Structure Observed by Swarm Satellites

Figure 1a shows as an example the MLAT versus time distribution of electron density of the ascending orbits of Swarm A from 15 April 2015 to 6 January 2016. The solar flux index, *f10.7* and the magnetic activity index, *Kp*, are also presented. These passes provide a 24 hours LT coverage starting at 17:00 LT during this period. From each ascending orbit of Swarm A the electron density data are sorted into MLAT bins with a size of 1°, and the coordinated universal time (UTC) at equator crossing is used for representing the epoch of the corresponding orbit. The EIA crests are clearly visible from 09:00 to 17:00 LT, with latitudes sometime extending to ±20° MLAT. From sunset to midnight hours, the two EIA crests are also seen, which move slightly away from the magnetic equator during PRE hours. Around midnight, the two peaks contract slowly back towards the magnetic equator and are sometimes still observed during postmidnight hours. Interestingly, two additional peaks appear from time to time at about ±40° MLAT (indicated by magenta arrows), and they are more prominent from midnight to sunrise hours. On the dayside, the electron density at low and the middle latitudes show a clear positive dependence on solar activity, for example, the 27-day variation, but not the electron density at night hours. In addition, enhanced electron density spikes are observed during higher magnetic activity periods. However, the two peaks at about ±40° MLAT during post-midnight hours show
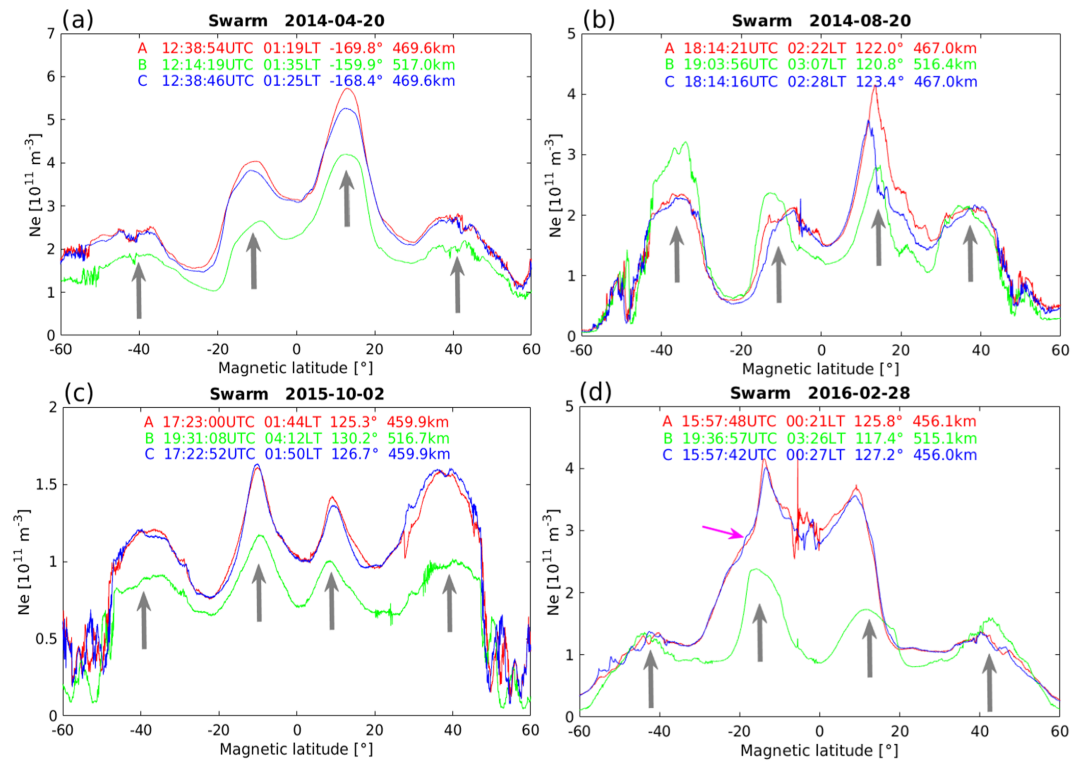
Figure 2. Examples of electron density profiles from four orbits of Swarm satellites. The Swarm B (green) revisits almost the same longitude of Swarm A (red) and C (blue), but with different time lags for the four examples: -20 min (earlier), 49 min, 128 min, and 219 min (later). The peaks of electron density are indicated by thick gray arrows. UTC = coordinated universal time.

no clear dependence on either the solar flux or magnetic activities. For example, they are observed at both lower (around 1 September) and higher (around 20 August) solar activity, as well as lower (around 2 October) and higher (around 19 September) magnetic activity periods.

To have a closer look at the four-peak latitudinal structure of electron density during magnetic quiet and disturbed periods, Figure 1b shows, as an example, one electron density profile of Swarm A from postmidnight hours on 2 October 2015 on magnetic quiet time (*Kp* was 2.3), and Figure 1c shows another example of Swarm A on 19 September 2015 on magnetic active time (*Kp* was 4.7). The UTC, LT, geographic longitude as well as the height when Swarm A passed the equator are given at the top of the figure. For both examples, the 2 Hz electron density measurements show clearly two peaks within $\pm 20°$ MLAT and the other two around $\pm 40°$ MLAT.

From Figure 1a (third panel), we see that the latitudinal four-peak structure of electron density can be observed throughout nighttime hours. However, Figure 1a highlights mainly the averages when condensing several months of Swarm A data in one plot. In fact, the orbital plane of Swarm B drifts slowly with a speed of 1.6 LT hours per year away from those of Swarm A/C. It means that Swarm B has the chance to resample the regions of Swarm A/C at a time difference that is increasing over the years. With this configuration, we can check the evolution of electron density peaks observed by Swarm A/C with Swarm B after a certain time delay.

Figure 2 presents four examples of electron density latitudinal profiles observed by the three Swarm satellites. In all the examples, four gray arrows mark the peaks. The four peaks in each example are generally located symmetrically about the magnetic equator, indicating a distribution along magnetic fluxtubes. During the first example on 20 April 2014 (shortly after completion of the constellation), Swarm B crossed the region of interest 24 min earlier than Swarm A/C, while in the other three examples Swarm B sampled the region later than the other two satellites by about 49 min, 128 min, and 219 min, respectively. In all the
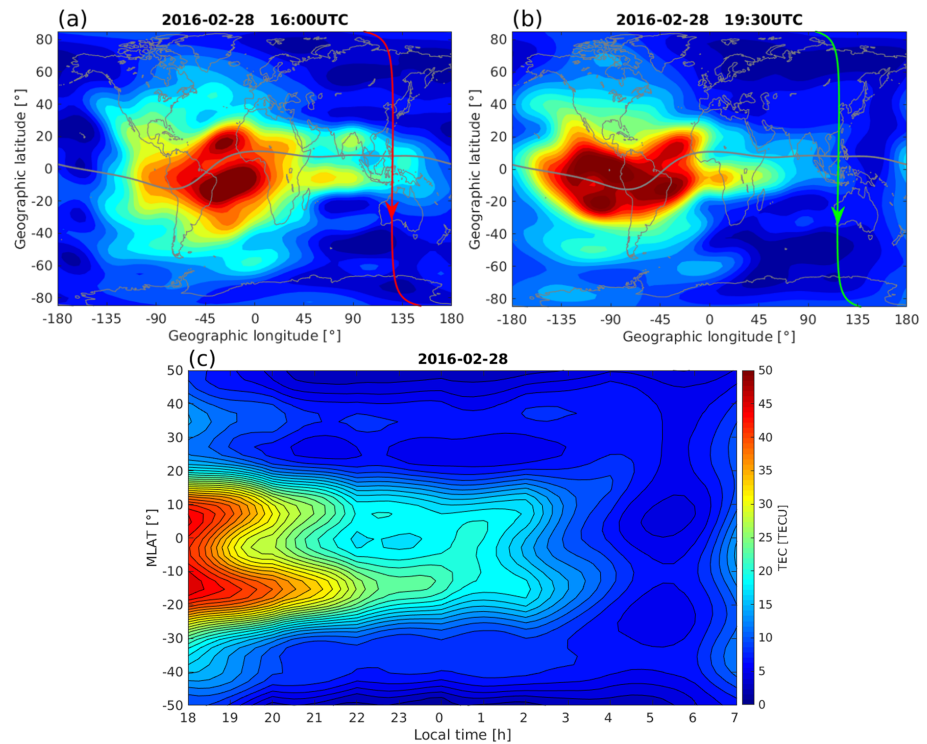
Figure 3. (a) The global total electron content (TEC) map at 16:00 coordinated universal time (UTC) on 28 February 2016. The red line indicates the descending orbit of Swarm A. (b) Similar as (a), but for the descending orbit of Swarm B. (c) The local time evolution of the TEC map around 120° E. TECU = total electron content unit.

examples, the longitudinal separation between the Swarm B and Swarm A/C sampled areas is less than 10°. It is no surprise to see that the electron density profiles observed by Swarm A and C are very similar, as the two spacecraft are flying side-by-side. But, it is interesting to see that the four peaks observed several hours later by Swarm B are located more or less at the same latitudes, especially for the two mid-latitude peaks at about ±40° MLAT. In the case of the two low-latitude peaks, they are found by all three Swarm satellites at quite the same latitudes for the examples in Figures 2a and 2c; while for the other two examples, the two low-latitude peaks are observed by Swarm B at locations even further away from the magnetic equator.

If we assume that the two low-latitude peaks are the remains of EIA from dusk side, they should appear closer to the magnetic equator at the Swarm B altitude, as Swarm B flies 50 km higher than the other two satellites and the westward electric field at the magnetic equator during late night hours is expected to cause a downward motion of the ionosphere. This contrary result suggests that the two low-latitude peaks observed by Swarm B in the examples 2b and 2d are possibly not the remnants of EIA from dusk hours. Another feature supporting this idea is that in Figure 2d the electron densities observed by Swarm A/C (around 00:21 LT) show clear shoulders at the mid-latitude flanks of the two EIA peaks. The shoulder, more prominent in the southern hemisphere at about −18° MLAT, is marked by a magenta arrow. About 3 h later (around 03:26 LT), Swarm B records the two low-latitude peaks right at the location of previously observed shoulders by Swarm A/C.

3.2. Global TEC Map Observations for the Example on 28 February 2016

In order to identify the detailed LT evolution of the latitudinal four-peak pattern, shown in Figure 2d, we check further the global TEC maps on that day. Figure 3a shows the TEC map for 16:00 UTC on 28 February 2016. The gray solid line marks the magnetic equator, and the red line indicates the descending orbit of Swarm A around 15:57 UTC. On the night side, the two crests of the EIA are discernable at about ±15° MLAT in the longitude sectors from 30° E to 135° E, corresponding to 18:00–24:00 LT. While from 120° E to 150° E, the two crests are located closer to the magnetic equator and seem to combine to one

peak in the TEC data. The TEC map in Figure 3a is in good agreement with the Swarm A electron density profile (shown in Figure 2d) around 00:21 LT and showing the two EIA crests equatorward of $\pm 15°$ MLAT. The two mid-latitude peaks, located close to $\pm 40°$ MLAT, are also visible from 30° E to $-135°$ E, corresponding to the nighttime hours from 18:00 LT to 07:00 LT. This indicates that the four-peak structures cover quite a large longitude region and are persistent from sunset to sunrise hours.

Similarly, Figure 3b shows the TEC map at 19:30 UTC, and the green line indicates the descending orbit of Swarm B around 19:36 UTC, recording the electron density as shown in Figure 2d. The enhanced crests of the EIA at PRE hours are seen in Figure 3b between $-45°$ E and 30° E, corresponding to the sector from 18:00 LT to 21:00 LT. The southern EIA crest is much stronger and extends to 60° E longitude, while the northern EIA crest is not discernable eastward of 30° E. However, two peaks appear again at low latitudes starting from 90° E longitude, and the two peaks appear progressively further away from the magnetic equator toward later LTs (more eastward). At longitudes around 120° E, the two peaks on the TEC map are located close to $\pm 20°$ MLAT, which corresponds well with the Swarm B electron density profile, as shown in Figure 2d. The two peaks located close to $\pm 40°$ MLAT are also visible in Figure 3b from 45° E to 135° E.

Figure 3c shows the LT evolution of the TEC map values from this day, focusing on longitudes around 120° E. For each 15 min UTC interval, the TEC values within a $\pm 5°$ longitude bin centered on 120° E, are averaged. From these bin averages, the latitude versus LT distribution of TEC values during postsunset hours is constructed. At low latitudes, the two EIA crests are enhanced from 18:00 LT. They reach latitudes furthest away from the magnetic equator around 21:00 LT. While from 21:00 to 22:00 LT, the two crests stay almost at the same latitude. After 22:00 LT, the northern crest disappears, but the southern is still observable until midnight. During post-midnight hours, the two peaks start to appear again and slowly move poleward, although the TEC magnitudes gradually decrease. The two peaks appearing around and during postmidnight hours seem not be related to the equatorial fountain effect, as the F region plasma drift is expected to be downward at the magnetic equator during postmidnight hours. We checked also the magnetic activity and AE indices, and found that Kp is less than 1, Dst is around 5 nT, AE is less than 200 nT on that day, therefore, no prominent eastward prompt penetration electric field from high latitudes is expected.

3.3. Statistical Properties of the Density Peaks

In a next step, we try to identify systematically the latitudinal four-peak electron density patterns in the Swarm nighttime orbits. For each Swarm orbit, a low-pass filter with cutoff scale-length of 2000 km is applied to the original data series to remove the small-scale variations. The peaks are then identified from the filtered data, and only the orbits with four peaks identified within $\pm 50°$ MLAT have been taken into account. In addition, we have utilized the special configuration of Swarm constellation that only the orbits, with electron density peaks first identified by Swarm A/C and then confirmed by the observations of Swarm B, have been taken into our statistics. The longitudinal separation between the areas sampled by Swarm A/C and Swarm B has been required to be less than 15°, and the derived density peaks should be closely located in latitude (less than 5°) between Swarm A/C and Swarm B observations. By applying these criteria, we have largely reduced false detection of other ionospheric structures, like the postsunset equatorial plasma irregularities (EPIs) and the travelling ionospheric disturbances (TIDs). Finally, 233 orbits were identified with latitudinal four-peak patterns in Swarm A/C observations, which are confirmed by Swarm B during the period from 18 April 2014 to 31 December 2018. This may be compared with the total number of over 50000 orbits of Swarm A satellite during this period. If we assume that Swarm A/C was in the favorable LT (22:00–04:00 LT) for only one fourth of the observation time and every second orbit of Swarm B passed close enough to the pair, we obtain an event detection rate of less than 4%. It is worth to mention that in this study only the latitudinal four-peak profiles observed by both Swarm A and B have been taken into account, which also means that if we consider observations from only one satellite, either Swarm A/C or B, such latitudinal four-peak events should have occurrence rate larger than 4%.

We have firstly checked the magnetic activity dependence of such latitudinal four-peak structure. Only few events are detected under magnetically disturbed periods (not shown here). The possible reason could be that during magnetically disturbed times the ionosphere is largely affected by the enhanced energy input from the solar wind/magnetosphere. Therefore, the latitudinal profile of electron density measured by Swarm satellites is expected to be more dynamic. In this way, the latitudinal four-peak structures are
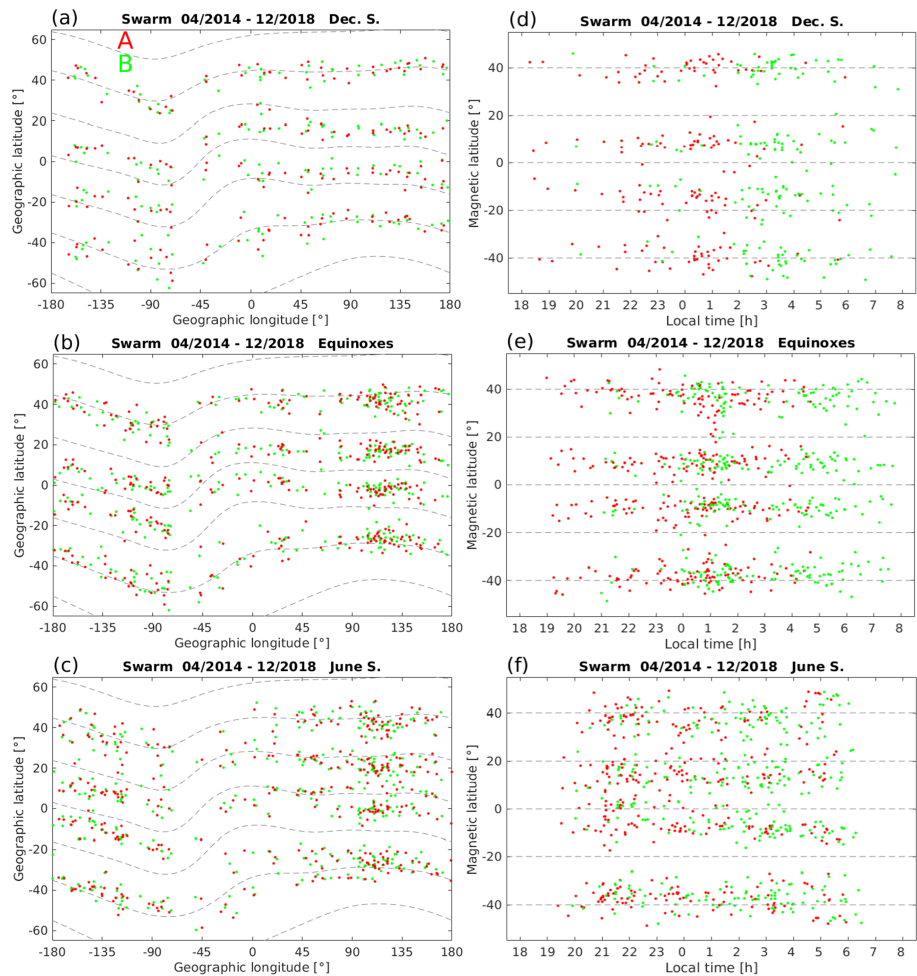
Figure 4. (a–c) The global distribution of four-peak events from Swarm A (red) and Swarm B (green) during three different seasons. The gray dashed lines are the magnetic contours between ±60° MLAT, with a step of 20°. (d–f) The magnetic latitude versus local time distribution of four-peak events.

easily erupted by the enhanced magnetically induced disturbances, like by large/medium-scale TIDs, as well as small-scale plasma irregularities. According to our approach, the latitudinal four-peak structure should be observed by both Swarm A/C and B. They sample the region of interest with a time separation from a few minutes to a few hours. That's why the latitudinal four-peak events, as shown in our study, are mainly detected at magnetically quiet period. Therefore, in the following, we have combined all the events regardless of magnetic as well as solar activities.

The global distributions of the electron density peaks observed by Swarm A (red) and B (green) are shown in Figures 4a–4c. As the results from Swarm C are practically identical with those of Swarm A, they are not shown here. The events have been divided into the three Lloyd seasons, and for each season the gray dashed lines in the figures are the MLAT contour lines from −60° to 60° with a step of 20°. The result shows that the two mid-latitude electron density peaks prefer to appear at latitudes close to ±40° MLAT at all three seasons, while the two low-latitude peaks show a slight seasonal dependence. For example, at equinoxes the two low-latitude peaks appear almost symmetrically about the magnetic equator, while during solstices the low-latitude peaks in the summer hemisphere are located at slightly higher latitudes. On global average, more events are observed in the eastern hemisphere between 90° E and 180° E longitudes.

The MLAT versus LT distributions of the electron density peaks are shown in Figures 4d–4f. The two mid-latitude peaks stay quite stable around ±40° MLAT during the night hours for all three seasons; while the two low-latitude peaks move slightly poleward from 02:00 LT to 06:00 LT during solstice seasons, but
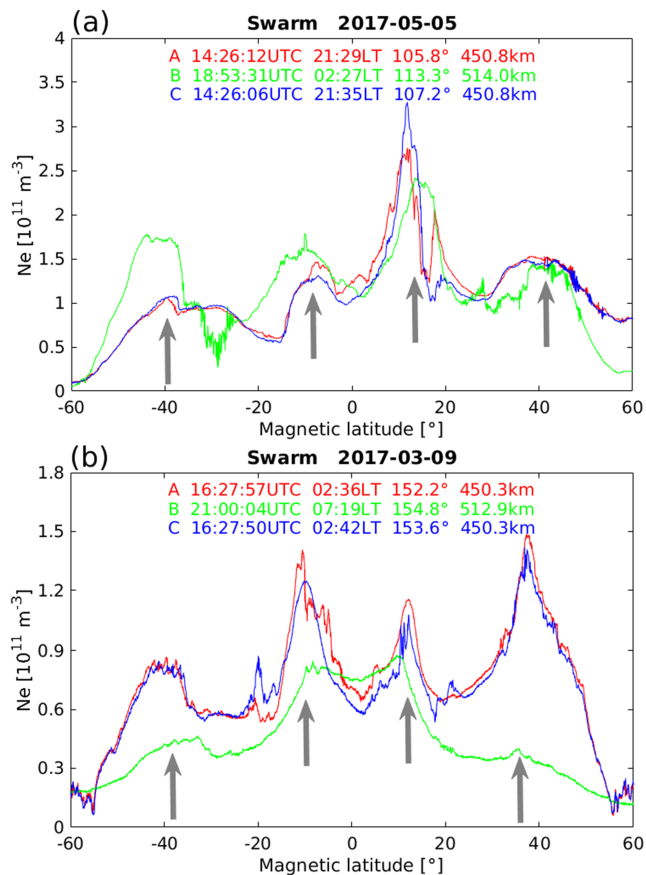
Figure 5. (a) One example of electron density profile when Swarm A/C passes around 21:30 local time (LT), a time when two equatorial ionization anomaly (EIA) crests are still prominent, while during the pass of Swarm B, 4 h and 27 min later (postmidnight), the four-peak pattern is evident. (b) Another example when Swarm A/C passes at postmidnight hours, while the pass of Swarm B, about 4 h 33 min later, shows a density profile from shortly after sunrise.

stays more or less at the same latitudes through equinoxes. After 06:00 LT, all the four peaks show a tendency of getting closer to the magnetic equator during December solstice and equinoxes.

At later years, the time difference in orbital planes between Swarm B and Swarm A/C satellites reaches almost 5 h. Therefore, we can check the evolution of the four peaks from premidnight to earlier morning or even after sunrise hours. Figure 5a provides one example when Swarm A/C observed two crests of the EIA one and a half hours before midnight, while 4 h and 27 min later, Swarm B observed two low-latitude peaks that are located further away from the magnetic equator, and the mid-latitude peaks are more prominent at this higher altitude. In the example of Figure 5b, Swarm B passed 4 h 33 min later than Swarm A/C, which is already in the postsunrise sector. Around 07:20 LT, the observed four peaks are much smaller, and all moved closer to the magnetic equator, which is consistent to the statistics shown in Figure 4. Another point we want to make is that in Figure 5b the two low-latitude peaks observed by Swarm B should not be related to the EIA crests so shortly after sunrise. The ion fountain needs several hours for lifting the plasma from the ionospheric E region to the topside F region at a 500 km altitude. They are more likely remnants of the two peaks observed by Swarm A/C at postmidnight hours but appearing closer to the magnetic equator at the higher altitude. We speculate that these two peaks will later be masked by the developing ionization anomaly. The two examples shown in Figure 5 suggest that the latitudinal four-peak structure can exist for several hours, persisting throughout the night until sunrise hours.

4. Discussions

In this study, we showed that the Swarm satellites sometimes observe latitudinal four-peak patterns of electron density along their orbits on the night side. The first explanation coming to mind is that the two low-latitude peaks are remains of the EIA crests from postsunset hours. It is true that the enhanced eastward electric field at the magnetic equator during PRE lifts the plasma to the topside ionosphere, and the plasma will stay there for several hours due to the relatively low recombination rate at higher altitudes. However, during the post-midnight hours, the westward electric field at the magnetic equator mainly causes a downward motion of the ionosphere, and the two EIA crests are expected to move closer to the equator. But as shown in both examples (Figures 2b and 2d) and statistical results (Figure 4), the EIA crests stay quite stable at the same latitude and even move further poleward during postmidnight hours.

Yizengaw et al. (2009) suggested that the postmidnight EIA signatures are caused by the reversed upward plasma drift, but are not the remnants of the dusk-side EIA. They explained that the positive gradient of the F region zonal neutral wind (increasing eastward velocity with LT) would result in an eastward electric field (Hari & Murthy, 1995), which then produces vertically upward drift velocity and causes the formation of EIA signatures in the postmidnight sector (Wang et al., 2008). However, the eastward zonal wind jet observed by the CHAMP satellite shows peak values around 20:00 LT (Liu et al., 2009), without clear positive gradient towards postmidnight hours. Therefore, the upward plasma drift reported by Yizengaw et al. (2009) during postmidnight hours might not be directly caused by the eastward electric field induced by the zonal wind gradient.

As shown in our Figure 2d, around postmidnight hours, the EIA crests (remnants from sunset hours) are still prominent. Meanwhile, clear shoulders already appear at the flanks of the two EIA crests, and the shoulders later develop into two new peaks when the previous EIA crests decay. This suggests that the driver for the shoulders (or peaks at a later LT observed by Swarm B) already exists when the dusk EIA still prevails around midnight hours. When the dusk EIA becomes weaker, this driver will dominate the latitudinal
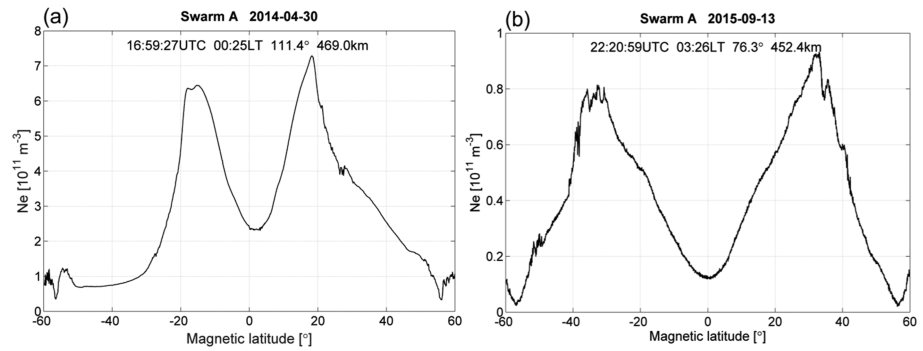
Figure 6. Examples of two-peak events appear at only (a) low latitudes and (b) middle latitudes, observed by both Swarm A. LT =local time.

distribution of *F* region electron density at post-midnight hours. As suggested by Titheridge (1995), the neutral wind plays a predominant role in the variation of *F* region electron density by lifting up or lowering the *F* region ionization. Therefore, the equatorward meridional winds at nighttime could be a possible candidate for this driver. Increased equatorward meridional winds at postmidnight hours can
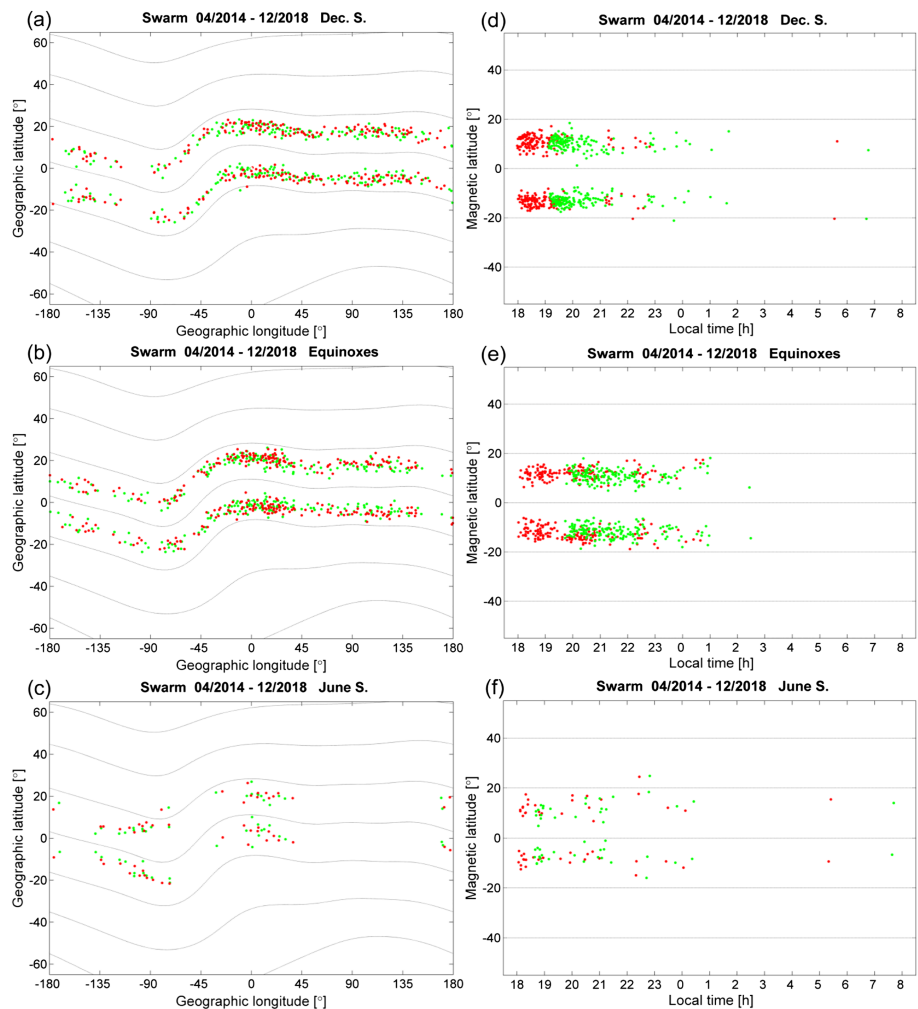

Figure 7. (a–c) The global distribution of the low-latitude two-peak events from Swarm A (red) and Swarm B (green) during three different seasons. The gray dashed lines are the magnetic contours between ±60° MLAT, with a step of 20°. (d–f) The magnetic latitude versus local time distribution of low-latitude two-peak events.
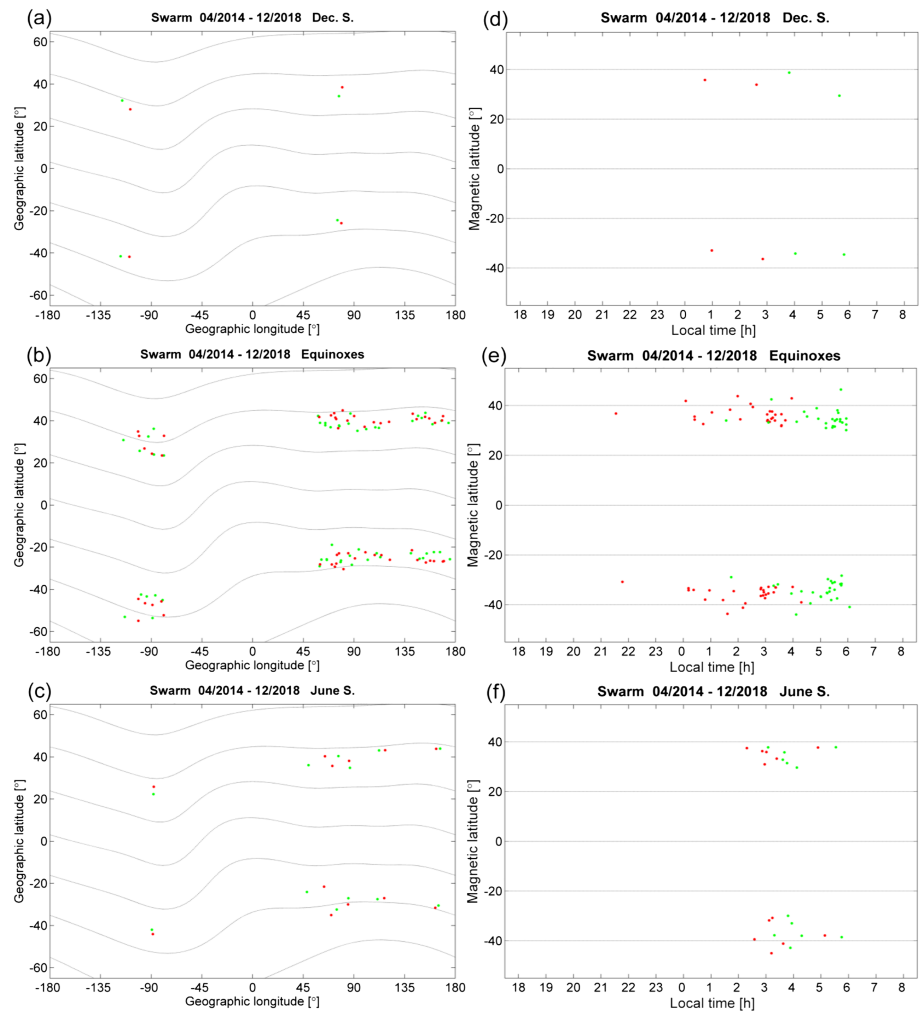
Figure 8. Similar as Figure 7, but for the events with two-peak events appear at middle latitudes.

push the plasma up along field lines and result in an upward component of plasma drift, due to the magnetic inclination of field lines at middle latitudes. The upward drifts will elevate the F2 layer and thus strongly decrease the efficiency of recombination, providing a sufficient plasma influx to start the electron density enhancement in the F2 region. As shown in Figure 3c, the newly formed two low-latitude peaks gradually shift to the northern hemisphere from 02:00 LT to 05:00 LT, which can be seen as an indicator for the meridional winds from summer to the winter hemisphere during postmidnight hours. Therefore, we suggest that the upward plasma drift induced by meridional wind dominates the formation of the two low-latitude peaks at post-midnight hours, and it could be more important than the effect of a reversed eastward electric field as proposed by Wang et al. (2008) and Yizengaw et al. (2009).

The neutral wind effect in fact depends on the actual configuration of the magnetic field, which can be expressed as (e.g., Liu et al., 2010):

$$W_{eff} = (V \cdot cosD \pm U \cdot sinD) \cdot cosI \cdot sinI, \tag{1}$$

where, U and V are the zonal and meridional wind components; D and I are the magnetic declination and inclination angles, respectively, and W_{eff} is the effective wind. By assuming a declination of 0°, the wind is most effective at an inclination of $\pm45°$. When considering a dipole magnetic field, the $\pm45°$ inclination occurs at $\pm26.6°$ MLAT, which are quite close to our two peaks at low latitude around $\pm20°$ MLAT. For the two middle latitude peaks, in addition to the meridional wind, other effects may contribute to the middle latitude electron density peaks at $\pm45°$ MLAT during nighttime, like downward diffusion from the
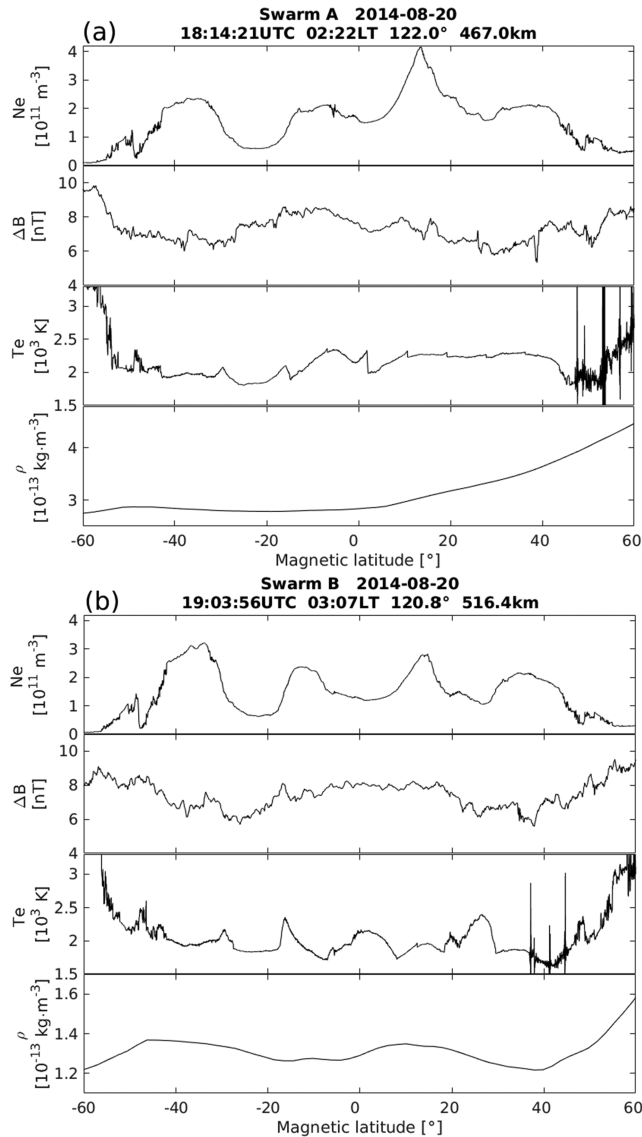
Figure 9. Comparison of latitudinal profiles for electron density, residual magnetic field strength, electron temperature, and neutral density, (a) from Swarm A and (b) from Swarm B satellites. The event is the same as shown in Figure 2b. LT = local time.

plasmasphere as suggested by Zhong et al. (2019). For low latitudes, we suggest that the actual location of the two electron density peaks depends on the competition between the dusk EIA fountain effect and the increasing equatorward winds at later LTs.

In this study we focus on the latitudinal four-peak structure in the nightside ionosphere, but the Swarm observations sometimes show only two peaks either at middle latitudes with absence of the two peaks at low latitude, or vice versa. Such examples are shown in Figure 6, and we see the two peaks appearing within (a) ±20° or (b) close to ±40° MLAT. Based on the Swarm electron density data set from April 2014 to December 2018, there are in total 312 and 34 events detected for the low-latitude and middle-latitude two-peak events, respectively. Their geographic latitude versus longitude, as well as MLAT versus local time distributions are shown in Figures 7 and 8. We see that for the low-latitude two-peak events almost all of them are observed from postsunset to midnight hours, indicating that they are mainly the remnant of the EIA from sunset. An interesting feature during Equinoxes is that the MLAT of the two peaks slightly shift to higher latitude from 00:00 LT to 01:00 LT, although there are only a few events. However, this feature is consistent with the local time variation of the four-peak structure event as shown in Figure 4. For the middle-latitude two-peak events, they mainly appear at postmidnight hours. Another feature worthy to be pointed out is that for the two-peak events appearing at low latitudes (Figure 7), they are symmetric about the magnetic equator during all three seasons. However, as shown in Figure 4, for the four-peak events, the two low-latitude peaks appear symmetric about the magnetic equator during equinoxes, while the peak in the summer hemisphere is found at slightly higher latitudes around solstice. This comparison suggests that the two low-latitude peaks of the four-peak events should have different drivers when compared to the EIA related two-peak events at low latitude.

By utilizing the Swarm constellation, we see that the four nighttime electron density peaks persist for several hours, therefore they have to be in pressure balance with the ambient. This means that the enhanced density has to be compensated by the reduction of another partial pressure term. For coming up with plausible suggestions it is helpful to take a look at the momentum equation. Since we are considering a stationary structure, we may ignore the inertial terms.

$$0 = \boldsymbol{j} \times \boldsymbol{B} + \nabla[n_e(T_e + T_i)]k_B - n_i m_i v_{in} \boldsymbol{V_i}, \qquad (2)$$

where, $\boldsymbol{j}$ is the ionospheric current; $\boldsymbol{B}$ is the magnetic field; n_e is the electron density; T_e and T_i are the electron and ion temperatures, respectively; k_B is the Boltzmann constant; n_i is the ion number density; m_i is the ion mass; v_{in} is the ion-neutral collision frequency, and $\boldsymbol{V_i}$ is ion velocity. Some of these terms can directly be tested with Swarm, for example, the $\boldsymbol{j} \times \boldsymbol{B}$ term, which is often referred to as diamagnetic effect. There are several examples in the literature where the diamagnetic effect provides the balance for plasma structures like the equatorial ionization anomaly (Lühr et al., 2003), postsunset equatorial plasma bubble (Stolle et al., 2006), or plasma irregularities at high latitudes (Laundal et al., 2019). Therefore, we would like to check if such relation is also valid for the four nighttime electron density peaks. The event shown in Figure 2b is taken as an example. For identifying the diamagnetic effect, the geomagnetic field contributions from the Earth's core, crust, and magnetosphere (here represented by the CHAOS-6 model, Finlay et al., 2015) have to be removed from the original Swarm magnetic measurements. By doing the subtraction, we isolate the magnetic field variations, B, originating from the ionosphere.

Figure 9 shows a comparison of electron density variations with three other simultaneously observed quantities: residual magnetic field strength, B, electron temperature, T_e, and mass density, ρ, from Swarm A and B. As can be deduced from the figure, no clear correlated variations of B are observed in relation to the electron density peaks for any of the two spacecraft. Therefore other quantities, like the plasma temperature or neutral density, may provide the pressure balance for these electron density peaks. Unfortunately, the quality of Swarm-measured electron and ion temperatures is poor. It is thus no surprise that no clear correlations with T_e can be found. And the low spatial resolution of the neutral density, ρ (about 10000 km), prevents from conclusive statements about its contribution to pressure balance. Further studies are encouraged for addressing this question and for identifying possible generation mechanisms.

5. Summary

In this study, we provide for the first time observations of the latitudinal four-peak structure of F region electron density in the nightside ionosphere, by using observations from the Swarm satellites. The main findings are summarized as:

1. The Swarm satellites sometimes observed latitudinal four-peak plasma density structures in the nightside ionosphere, which can last from premidnight to sunrise hours. The two mid-latitude peaks prefer to appear at $\pm 40°$ MLAT, while two low-latitude peaks appear within $\pm 20°$ MLAT. Such latitudinal four-peak structures can persist throughout the night until sunrise hours.
2. No clear seasonal dependence is found for the two mid-latitude peaks. The two low-latitude peaks appear almost symmetric about the magnetic equator during equinoxes, while around solstices the peak in the summer hemisphere is shifted to slightly higher latitudes.
3. The two low-latitude peaks at late-night hours are believed not to be remnants of the dusk-side EIA crests, as (a) an example shows that Swarm A/C observes the development of shoulders at the flanks of the two EIA crests after sunset hours, and the shoulders become peaks 3 h later when Swarm B resamples the same region;(b) statistic results reveal that the two low-latitude peaks during post-midnight hours do not propagate towards the magnetic equator, as expected for EIA crests, but move slowly poleward. We suggest that the enhanced meridional wind at post-midnight hours is an important driver for causing such long-lasting latitudinal four-peak structures of F region electron density.
4. Pressure balance within these density peaks is not maintained by a reduced magnetic field (diamagnetic effect). Other quantities, like plasma temperature, might vary accordingly to maintain the structures stationary, which encourages further investigation.

References

Appleton, E. V. (1946). Two anomalies in the ionosphere. *Nature*, *157*(3995), 691. https://doi.org/10.1038/157691a0

Arendt, P. R., & Soicher, H. (1964). Downward electron flux at 1000 km altitude from electron content measurement at mid-latitudes. *Nature*, *204*(4962), 983–984. https://doi.org/10.1038/204983a0

Balan, N., & Rao, P. B. (1987). Latitudinal variations of nighttime enhancements in total electron content. *Journal of Geophysical Research*, *92*(A4), 3436–3440. https://doi.org/10.1029/JA092iA04p03436

Duncan, R. A. (1959). The equatorial F-region of the ionosphere. *Journal of Atmospheric and Terrestrial Physics*, *18*(2-3), 89–100. https://doi.org/10.1016/0021-9169(60)90081-7

Eccles, J. V., Maurice, J. P. S., & Schunk, R. W. (2015). Mechanisms underlying the prereversal enhancement of the vertical plasma drift in the low-latitude ionosphere. *Journal of Geophysical Research: Space Physics*, *120*, 4950–4970. https://doi.org/10.1002/2014JA020664

Feltens, J., & Schaer, S. (1998). IGS Products for the Ionosphere. In J. M. Dow, J. Kouba, & T. Springer (Eds.), *Proceedings of the IGS Analysis Center Workshop* (pp. 225–232). Darmstadt.

Finlay, C. C., Olsen, N., & Tøffner-Clausen, L. (2015). DTU candidate field models for IGRF-12 and the CHAOS-5 geomagnetic field model. *Earth, Planets and Space*, *67*, 157–189. https://doi.org/10.1186/s40623-015-0274-3

Hari, S. S., & Murthy, B. V. K. (1995). Seasonal variations of equatorial night-time thermospheric meridional winds. *Journal of Atmospheric and Solar - Terrestrial Physics*, *57*, 1241–1246. https://doi.org/10.1016/0021-9169(95)00007-O

Jakowski, N., & Förster, M. (1995). About the nature of the nighttime winter anomaly effect. *Planetary and Space Science*, *43*(5), 603–612. https://doi.org/10.1016/0032-0633(94)00115-8

Kelley, M. C. (2009). *The Earth's ionosphere: Electrodynamics and plasma physics* (2nd ed.). New York: Elsevier.

Laundal, K. M., Hatch, S. M., & Moretto, T. (2019). Magnetic effects of plasma pressure gradients in the upper F region. *Geophysical Research Letters*, *46*, 2355–2363. https://doi.org/10.1029/2019GL081980

Li, Z. S., Ning-Bo, W., Min, L., Kai, Z., Yun-Bin, Y., & Hong, Y. (2017). Evaluation and analysis of the global ionospheric TEC map in the frame of international GNSS services. *Chinese Journal of Geophysics (in Chinese)*, *60*(10), 3718–3729. https://doi.org/10.6038/cjg20171003

Liang, P. H. (1947). F2 ionization and geomagnetic latitudes. *Nature*, *160*(4071), 642–643. https://doi.org/10.1038/160642a0

Liu, H., Stolle, C., Förster, M., & Watanabe, S. (2007). Solar activity dependence of the electron density in the equatorial anomaly regions observed by CHAMP. *Journal of Geophysical Research*, *112*, A11311. https://doi.org/10.1029/2007JA012616

Liu, H., Thampi, S. V., & Yamamoto, M. (2010). Phase reversal of the diurnal cycle in the midlatitude ionosphere. *Journal of Geophysical Research*, *115*, A01305. https://doi.org/10.1029/2009JA014689

Liu, H., Watanabe, S., & Kondo, T. (2009). Fast thermospheric wind jet at the Earth's dip equator. *Geophysical Research Letters*, *36*, L08103. https://doi.org/10.1029/2009GL037377

Lühr, H., Rother, M., Maus, S., Mai, W., & Cooke, D. (2003). The diamagnetic effect of the equatorial Appleton anomaly: Its characteristics and impact on geomagnetic field modeling. *Geophysical Research Letters*, *30*(17), 1906. https://doi.org/10.1029/2003GL017407

McDonald, S. E., Dymond, K. F., & Summers, M. E. (2008). Hemispheric asymmetries in the longitudinal structure of the low-latitude night time ionosphere. *Journal of Geophysical Research*, *113*, A08308. https://doi.org/10.1029/2007JA012876

Mikhailov, A. V., Förster, M., & Leschinskaya, T. Y. (2000). On the mechanism of the post-midnight winter NmF2 enhancements: Dependence on solar activity. *Annales de Geophysique*, *18*(11), 1422–1434. https://doi.org/10.1007/s00585-000-1422-y

Namba, S., & Maeda, K. I. (1939). Radio wave propagation (pp. 86). Corona, Tokyo.

Stolle, C., Lühr, H., Rother, M., & Balasis, G. (2006). Magnetic signatures of equatorial spread F as observed by the CHAMP satellite. *Journal of Geophysical Research*, *111*, A02304. https://doi.org/10.1029/2005JA011184

Titheridge, J. E. (1995). Winds in the ionosphere – A review. *Journal of Atmospheric and Terrestrial Physics*, *57*(14), 1681–1714. https://doi.org/10.1016/0021-9169(95)00091-F

Wang, W., Lei, J., Burns, A. G., Wiltberger, M., Richmond, A. D., Solomon, S. C., et al. (2008). Ionospheric electric field variations during a geomagnetic storm simulated by a coupled magnetosphere ionosphere thermosphere (CMIT) model. *Geophysical Research Letters*, *35*, L18105. https://doi.org/10.1029/2008GL035155

Woodman, R. F. (1970). Vertical drift velocities and East-West electric fields at the magnetic equator. *Journal of Geophysical Research*, *75*(31), 6249–6259. https://doi.org/10.1029/JA075i031p06249

Xiong, C., Lühr, H., & Ma, S. Y. (2013). The magnitude and inter-hemispheric asymmetry of equatorial ionization anomaly-based on CHAMP and GRACE observations. *Journal of Atmospheric and Terrestrial Physics*, *105-106*, 160–169. https://doi.org/10.1016/j.jastp.2013.09.010

Xiong, C., Stolle, C., Lühr, H., Park, J., Fejer, B. G., & Kervalishvili, G. N. (2016). Scale analysis of the equatorial plasma irregularities derived from Swarm constellation. *Earth, Planets and Space*, *68*(1), 1–12. https://doi.org/10.1186/s40623-016-0502-5

Yeh, K. C., Franke, S. J., Andreeva, E. S., & Kunitsyn, V. E. (2001). An investigation of motions of the equatorial anomaly crest. *Geophysical Research Letters*, *28*(24), 4517–4520. https://doi.org/10.1029/2001GL013897

Yizengaw, E., Moldwin, M. B., Sahai, Y., & de Jesus, R. (2009). Strong postmidnight equatorial ionospheric anomaly observations during magnetically quiet periods. *Journal of Geophysical Research*, *114*, A12308. https://doi.org/10.1029/2009JA014603

Zhong, J., Lei, J., Yue, X., Luan, X., & Dou, X. (2019). Middle-latitudinal band structure observed in the nighttime ionosphere. *Journal of Geophysical Research: Space Physics*, *124*, 5857–5873. https://doi.org/10.1029/2018JA026059